J. Braz. Chem. Soc., Vol. 18, No. 5, 1017-1023, 2007.
Printed in Brazil - ©2007 Sociedade Brasileira de Química
0103 - 5053 $6.00+0.00

Article

Assembling of Xyloglucans and Lectin onto Si Wafers and onto Amino-Terminated Surfaces

Maria Rita Sierakowski,[a] Lizandra B.R.Castro,[b] Neoli Lucyszyn[a] and Denise F. S. Petri[*,b]*

[a]*Laboratório de Biopolímeros, Departamento de Química, Universidade Federal do Paraná, CP 19081, 81531-990 Curitiba-PR, Brazil*

[b]*Instituto de Química, Universidade de São Paulo, CP 26077, 05513-970 São Paulo-SP, Brazil*

A imobilização de xiloglucanas (XG) extraídas de sementes de *Hymenaea coubaril* (HXG) e de *Tamarindus indica* (TXG) sobre lâminas de Si/SiO_2 ou lâminas modificadas com grupos amina a partir de solução aquosa na concentração de 0,5 g L^{-1} e em pH 3,5 foi investigada através de elipsometria e medidas de microscopia de força atômica (AFM). Os experimentos foram feitos sob condições de equilíbrio (adsorção) ou de não equilíbrio (evaporação do solvente). Sob condições de equilíbrio as cadeias de HXG e TXG não adsorvem sobre lâminas de Si/SiO_2, indicando que os grupos SiO^- na superfície não interagem com as mesmas. Camadas de TXG e HXG obtidas sobre lâminas de Si/SiO_2 por evaporação do solvente apresentaram espessuras de (2,4 ± 0,4) nm e (3,8 ± 0,9) nm, respectivamente. Cadeias de TXG e HXG adsorveram sobre lâminas modificadas com grupos amina formando filmes com (1,0 ± 0,1) nm e (1,3 ± 0,1) nm de espessura, respectivamente. Após evaporação do solvente sobre lâminas modificadas com grupos aminas, formaram-se agregados e fibrilas de TXG e HXG, os quais aumentaram os valores médios de espessura e rugosidade. Independentemente do tipo de substrato, cadeias de HXG tenderam a formar camadas mais espessas que cadeias TXG. Esta tendência foi explicada com base nas características moleculares das cadeias de HXG, como por exemplo, massa molar e tamanho de persistência maiores. As isotermas de adsorção de concanavalina A (Con A) sobre TXG e HXG adsorvidas sobre lâminas modificadas com grupos amina apresentaram valor máximo de (3,3 ± 0,3) mg m^{-2}. Imagens de AFM mostraram moléculas de Con A densamente empacotadas sobre as superfícies de TXG e HXG. Fibrilas e agregados foram observados somente quando as superfícies de TXG e HXG foram preparadas por evaporação do solvente. Nesta situação, as moléculas de Con A adsorveram predominantemente sobre regiões livres de fibrilas e agregados.

Immobilization of xyloglucans extracted from *Hymenaea coubaril* (HXG) and *Tamarindus indica* seeds (TXG) on Si/SiO_2 wafers or amino-terminated wafers from aqueous solution at concentration of 0.5 g L^{-1} and pH 3.5 has been investigated by means of ellipsometry and atomic force microscopy (AFM) measurements. Experiments were carried out under equilibrium conditions (adsorption) and non-equilibrium conditions (casting). Under equilibrium conditions neither TXG nor HXG chains adsorbed from solution onto Si/SiO_2 surfaces, indicating that negatively charged SiO^- groups on the surface do not attract XG chains. Casting TXG and HXG solutions onto Si/SiO_2 surfaces led to layers (2.4 ± 0.4) nm and (3.8 ± 0.9) nm thick, respectively. TXG and HXG adsorbed onto amino-terminated surfaces forming layers (1.0 ± 0.1) nm and (1.3 ± 0.1) nm thick, respectively. Upon casting solutions of TXG and HXG onto amino-terminated surfaces, aggregates and fibrils appeared more frequently on the surface, increasing the mean thickness and roughness values. Regardless the substrate, HXG chains tended to form thicker layers than TXG chains did. This trend can be explained with basis on the molecular characteristics of HXG, namely, higher molecular weight and persistence length. The adsorption isotherms of concanavalin A (Con A) onto HXG- and TXG-covered amino-terminated wafers presented maximum adsorbed amount of (3.3 ± 0.3) mg m^{-2}. AFM images shown Con A molecules as small entities densely packed on the surface. The presence of fibrils and aggregates was observed only when the TXG and HXG surfaces were prepared by casting. There ConA molecules adsorbed predominantly on regions free of fibrils and aggregates.

Keywords: xyloglucans, concanavalin A, thin films, atomic force microscopy, ellipsometry

*e-mail: dfsp@iq.usp.br

Introduction

Xyloglucans (XG) are hemicellulosic polysaccharides found in the cell wall of all higher plants. Xyloglucan (XG) has (1→4)-β-D-glucopyranan backbone decorated with α-D-xylopyranose residues or β-D-galactopyranose (1→2)-α-D-xylopyranose oligomer at position 6.[1,2] The effect of XG structural features such as molecular weight and side chain residues on the XG-cellulose interaction has been recently explored.[3-8] Binding XG to cellulose is favored when XG molecular weight decreases[4] or when a certain pattern of galactosyl branches is present.[3] Force spectroscopy between XG modified atomic force microscopy (AFM) tip and cellulose substrates indicated adhesion forces in the range of 25 – 70 pN. [5] Geometrical details about the adsorption of XG onto cellulose surfaces and the effect of the lateral chain size on the binding have been described by means of molecular dynamics simulations,[8] which indicated that the adsorption XG is not specific; it takes place when XG backbone has parallel, perpendicular and anti-parallel orientations. Moreover, XG interacts with cellulose via side chains as well as via backbone. XG with short side chains tends to adapt itself to the cellulose microfibril, adsorbing flat on the cellulose surface. The same is not observed for XG with long side chains. Understanding the adsorption behavior of XG onto cellulose surfaces has potential applications for the pulp and paper industry,[6,7] for instance, it has been shown that XG covered cellulose surfaces repel each other, reducing friction.[7] While the adsorption of XG onto flat cellulose surface has been well described, the formation of XG films onto flat SiO_2 surfaces has been seldom investigated. Such flat surfaces are very useful for the construction of biosensors and kits for analytical tests. A quick survey showed that there is only a patent about this subject.[9] In this work assembling of XG extracted from seeds of *Hymenaea coubaril* and *Tamarindus indica*, onto Si/SiO_2 wafers and amino-terminated surfaces has been studied by means of ellipsometry and atomic force microscopy (AFM). The immobilization of a lectin, Concanavalin A, onto XG-covered wafers was also investigated, since lectins are proteins that specifically interact with carbohydrates, playing a prominent role *e.g.* for cell adhesion and recognition of pathogens by specific surface carbohydrates by the immune system, and can be useful probes in studying carbohydrates of cell surfaces. Apart from their physiological importance, carbohydrates and lectins are also expected to become important tools for recognition of bioanalytes[11] or drug targeting.[12]

Experimental

XG samples extracted from seeds of *Hymenaea coubaril* (Fortaleza, CE) and *Tamarindus indica (*Teodoro Sampaio, Ba) containing near of 3% protein were coded as HXG and TXG, respectively. Sample characteristics are shown in Table 1. Concanavalin A (Con A), type IV, from *canavalia ensiformis* (M_w of 25583 g mol^{-1}, Sigma C2010, USA), was used without any purification. Silicon wafers (Si/SiO_2) purchased from SiliconQuest, USA, were rinsed in a standard manner[13,14] prior to the XG adsorption. Amino-terminated wafers were prepared by reaction with aminopropyltriethoxy silane (APS, Acros, USA).[13,14]

Table 1. Characteristics of HXG and TXG. Weight average molecular weight, M_w, (g mol^{-1}), number average molecular weight, M_n, (g mol^{-1}) radius of gyration, R_g, (nm), and persistence length (L_p) determined by means of size exclusion chromatography and light scattering measurements[10]

Sample	M_w	M_n	M_w/M_n	R_g	L_p/(nm)
HXG	2.2×10^6	1.5×10^6	1.4	110.4	10.9 ± 0.2
TXG	1.1×10^6	7.2×10^5	1.5	68.6	6.2 ± 0.2

Thin film formation of XG onto Si wafers and onto amino-terminated surfaces was performed from XG solution 0.5 g L^{-1}, at pH 3.5, following two different strategies. In the first one, the substrates were dipped into XG solutions at (24 ± 1) °C, where XG samples were allowed to adsorb under equilibrium conditions. After 12h they were removed from XG solution, washed 10 times in distilled water, dried under a stream of N_2 and characterized. In the second method, a 10 μL drop of each XG solution was cast on the surfaces and allowed to evaporate at (24 ± 1) °C and 60% of relative humidity. Then the substrates were immersed in distilled water during 24h (in order to remove the physically adsorbed XG), dried under a stream of N_2 and characterized. The XG solutions were prepared at pH 3.5 because at this pH amino-terminated surfaces carry many positive charges ($-NH_3^+$)[14] and Si/SiO_2 many negative charges (SiO^-).[15,16] One should remember that pK_b for propylamino groups is reported[14] to be 3.3 and the isoelectric point of silica is close too 3.0[15,16] at the temperature of 20 °C. The subsequent adsorption of Con A onto XG covered substrates was performed from Con A solutions in the concentration range of 0.01 to 0.6 g L^{-1}, at pH 4.5, in the presence of $MnCl_2$ and $CaCl_2$ 0.01 mol L^{-1} during 3h, at (24 ± 1) °C. Specific binding of Con A to glucose or mannose monomers requires the presence of Mn^{2+} and Ca^{2+} ions.[17,18]

Ellipsometry

Ellipsometric measurements were performed *ex-situ* using a vertical computer-controlled DRE-EL02 Ellipsometer (Ratzeburg, Germany). The angle of incidence was set to 70.0° and the wavelength of the laser was 632.8 nm with an incidence area of 3 mm^2. For the interpretation of the ellipsometric angles Δ and Ψ a multilayer model was used, considering refractive index n for Si, 3.88 – 0.018i; for SiO_2, 1.462; for APS, 1.424; for XG layer, 1.500; for Con A layer 1.520, and for air 1.000. The thickness of adsorbed XG layer can be calculated by iteractive calculations with Jones matrices.[19,20] Each layer is usually characterized sequentially regarding independent ellipsometric determinations of thickness and refractive index.[19,20] One should also notice that ellipsometry enables the independent determination of n and d, only if the optical contrast in the system is large enough or if the layer thickness is thick enough. When λ is 633 nm and d >> 30 nm, it is possible to obtain n and d for the uppermost layer independently. However, in the present system, d << 30 nm for the uppermost polymer layer, so that n must be assumed as n = 1.500, the usual value for a polysaccharide layer, and d calculated from ellipsometric angles and the multilayer model plus independent determinations of thicknesses and refractive indices for each layer. Similarly, the thickness of Con A layer was calculated, considering the refractive index of 1.520, a typical value for proteins. Ellipsometric measurements were always performed on three different areas of the same sample in order to have information about film homogeneity. The mean thickness values are mean values of duplicates or triplicates. The corresponding standard deviations indicate the film homogeneity and reproducibility.

The adsorbed amount of ConA onto XG-covered surfaces Γ_{ConA} was estimated by

$$\Gamma_{ConA} = d_{ConA} \cdot \rho \quad (1)$$

where ρ is the density of a dry protein layer ($\rho \sim 1.37$ g cm^{-3}).[21]

Atomic Force Microscopy (AFM)

Atomic Force Microscopy (AFM) measurements were performed in a PicoSPM LE (Molecular Imaging) microscope in the intermittent contact mode in air at (24 ± 1) °C. The cantilevers operated slightly below their resonance frequency of approximately 290 kHz. All topographic images represent unfiltered original data. At least two samples of the same material were analyzed at different areas of the surface. The root mean square (r.m.s.) roughness values were calculated for substrates scan areas of 1 μm × 1 μm.

Results and Discussion

Immobilization of TXG and HXG onto Si/SiO_2 wafers

Table 2 shows mean thickness (d) of layers formed by immobilizing TXG and HXG onto Si/SiO_2 wafers, as determined by means of ellipsometry and the corresponding mean surface roughness (rms) values, as determined from topographic images and PicoScan 5.3.2. software. Such techniques are powerful tools for the characterization of thin films.[22] Under equilibrium conditions XGs did not adsorb from solution onto Si/SiO_2 surfaces, indicating that negatively charged SiO^- groups on the surface do not attract XG chains. Interestingly, TXG and HXG formed films by casting onto Si/SiO_2 surfaces with mean thickness of (2.4 ± 0.4) nm and (3.8 ± 0.9) nm, respectively. By casting the solvent evaporates slowly, forcing polymer chains to remain on the substrate. Immobilized HXG chains led to layers ~50% thicker than those formed by TXG. This finding might be explained with basis on HXG mass-average molar mass, M_w, which is twice TXG M_w. Although TXG and HXG layers are not perfectly homogeneous, as considered in the model used for calculations, the laser spot area of 3 mm^2 is much larger than the mean roughness (rms) values (Table 2), making the comparison between the d values reliable. Desorption experiments were performed by dipping HXG and TXG covered-wafers into pure water for 24 hours. After that period of time, the samples were removed and dried. After desorption experiments ellipsometric measurements were again performed on three different areas of the same sample. Negligible changes in mean thickness values have been observed, indicating that the immobilization of TXG and HXG is irreversible. Changes in mean thickness values were considered negligible because they were similar or smaller than the standard deviations calculated. Upon solvent evaporation a larger number of silanol (SiOH) groups might appear on the surface, which is able to interact with XG hydroxyl groups by hydrogen bond. One should notice that both cellulose and Si/SiO_2 surfaces are -OH rich. Molecular dynamics simulations[8] showed that each XG molecule forms no more than four hydrogen bonds upon adsorbing onto cellulose surface and that such hydrogen bonds are not the determinant factor for the association between XG and

cellulose; van der Waals and electrostatic contributions should be also considered.

HXG and TXG formed layers with irregular topography, as shown in Figures 1a and 1c, respectively. However, HXG surfaces are smoother than TXG, as evidenced by the cross section analyses and rms values (Table 2). Fine structures of HXG and TXG are different.[10] Only HXG samples present the nonasaccharide XXXXG (4 xylose (X) and 5 glucose (G) units) in its composition, which lead to high persistence length[10] (Table 1) and might favor spreading of chains on the Si wafers. AFM images (not shown) taken after desorption experiments presented similar features.

Figures 1b and 1d are phase images obtained for HXG and TXG layers, respectively. The main information one obtains from phase images is the dissipation of the cantilever oscillation in that point. Contrast in the phase image means different amount of dissipation. This can both arise from a change in material or a change in interaction geometry. Therefore, topography and differences in material characteristics (softness/stickiness/damping) might contribute to phase contrast. In some cases it might be hard to separate both contributions. Edges or steep slopes definitely contribute to phase image. On the other hand, height differences between flat areas should not cause a difference in phase.[23] Phase images in Figures 1b (HXG) and 1d (TXG) showed low contratst, which compared to the topography, indicated small material contrast, and therefore, large surface coverage in both cases.

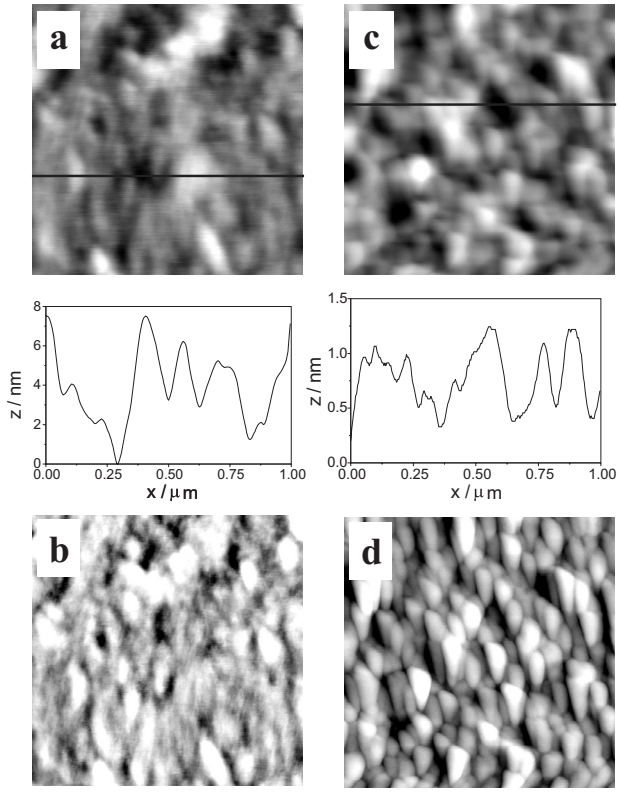

Figure 1. AFM images 1 μm × 1 μm: (a) topography (z =3 nm) with the corresponding cross section analysis and (b) phase image (z = 2 V) of HXG cast onto Si/SiO_2 surfaces; (c) topography (z = 8 nm) with the corresponding cross section analysis and (d) phase image (z = 1 V) of TXG cast onto Si/SiO_2 surfaces.

Immobilization of TXG and HXG onto amino-terminated wafers

TXG and HXG adsorbed from aqueous solution onto amino-terminated substrates forming layers with similar mean d and rms values (Table 2), indicating that XG source or fine structure played no role in this case. HXG and TXG (Figure 2a) formed small aggregates and fibrils on the amino-terminated surfaces. The contour lengths of fibrils ranged from 110 nm to 360 nm. Similar features have been observed for TXG on mica.[5] Fibrils are ~3.0 nm high (cross-sections), indicating that the fibrils might be composed by bundle of few XG chains. Regardless the XG, the adhesion of TXG or HXG onto amino-terminated was irreversible. Dipping the XG-covered surfaces into distilled water for 24 hours was not able to remove the

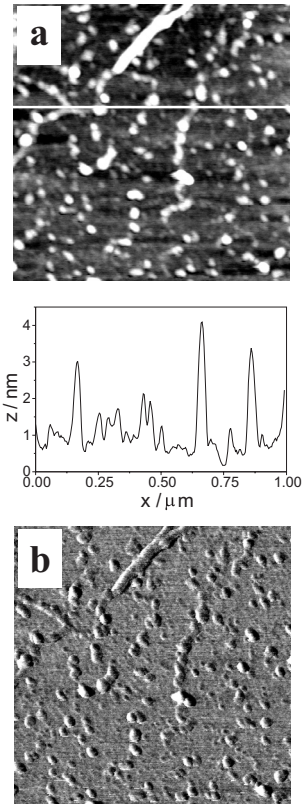

Figure 2. AFM images 1 μm × 1 μm obtained for HXG adsorbed onto amino-terminated surfaces (a) topography (z = 3 nm) with the corresponding cross-section analysis and (b) phase image (z = 2 V).

adsorbed material. No changes in thickness or morphology of XG-covered wafers could be observed. Phase image (Figure 2b) showed some contrast, which might be attributed to topography and material contrast, since brighter contrast might be due to stiffer material or higher structure.

XG layers deposited onto amino-terminated surfaces by casting were thicker than those layers formed by adsorption (Table 2). HXG and TXG layers presented similar morphological features, as evidenced in Figures 3a and 3c, respectively. The presence of large aggregates brought about the apparent increase in thickness and rms values. Fibrils ~ 3.0 nm high with contour lengths varying from 180 nm to 900 nm could be observed. Such dimension might be attributed to bundles of XG chains. Upon immerging XG coated surfaces into pure water for 24 hours, about 50% of desorption was observed, indicating that many TXG or HXG chains were weakly attached to the surface or to the other XG chains. Even after desorption, HXG layers remained thicker than TXG layers. Again, this finding might be explained with basis on HXG M_w, which is twice TXG M_w. Brighter contrast in phase images (Figures 3b and 3d) might be attributed to topography and material contrast, since brighter contrast might be due to stiffer material or higher structure. The presence of aggregates and fibrils at both mica[5] (negative charged in solution) and at amino terminated surfaces (positive charges) were observed when the layers were cast under non-equilibrium condition and when adsorption took place (equilibrium condition). Uncharged polysaccharides tend to aggregate because of the strong tendency to form intermolecular H bonding, regardless the substrate charge.

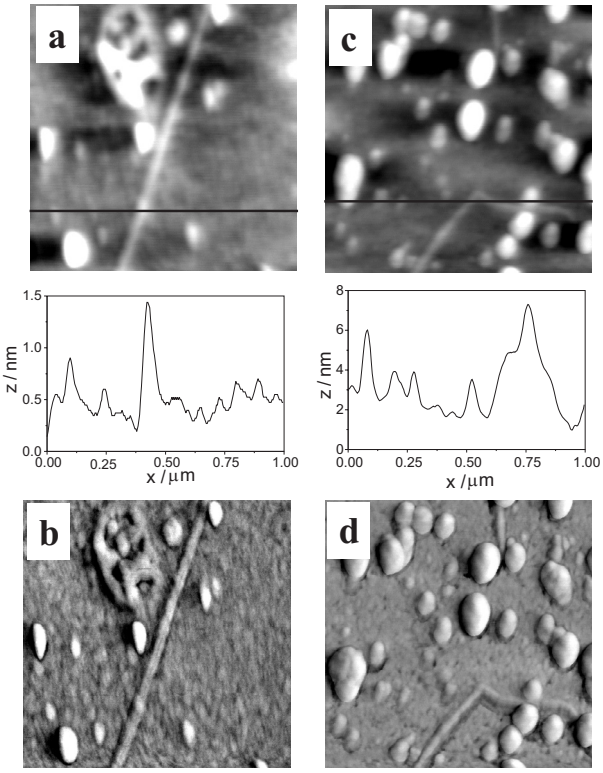

Figure 3. AFM images 1 μm × 1 μm: (a) topography (z = 2.5 nm) with the corresponding cross-section analysis and (b) phase image (z = 0.3 V) of HXG cast onto amino-terminated surfaces; (c) topography (z = 12 nm) with the corresponding cross-section analysis and (d) phase image (z = 1.5 V) of TXG cast onto amino-terminated surfaces.

Adsorption of ConA onto XG films

Since immobilization of HXG and TXG chains was more efficient onto amino-terminated wafers, they have been chosen as substrates for the Con A adsorption experiments under equilibrium-conditions. Figure 4 shows the adsorption isotherms of Con A onto HXG or TXG previously adsorbed onto amino-terminated wafers. The adsorbed amount Γ increased linearly with Con A concentration until a maximum Γ value of (3.3 ± 0.3) mg m^{-2}, which corresponds to the mean thickness of (2.4 ± 0.3) nm. This is less than the size of a monomer of the lectin estimated to be a dome-shaped molecule of 4.2 × 4.0 × 3.9 nm.[24] A similar behavior was observed for the adsorption of Con A onto bare Si/SiO_2 wafers.[25] In both cases, the surface coverage seems to be incomplete. Typical AFM topographic images of Con A onto HXG, TXG cast and TXG adsorbed onto amino-terminated surfaces are presented in Figures 5a, 5c and 5e, respectively, with the corresponding cross section analyses. For AFM analyses Con A molecules were allowed to adsorb under equilibrium conditions during three hours at the concentration of 0.2 g L^{-1}. All images show ConA molecules as small globular entities packed on the surface. Similar features were observed for ConA

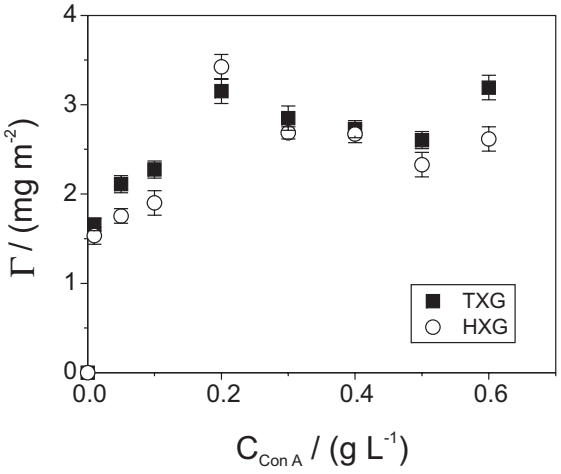

Figure 4. Adsorption isotherms of Con A onto TXG (solid squares) and HXG (open circles) covered surfaces determined at (24 ± 1) °C.

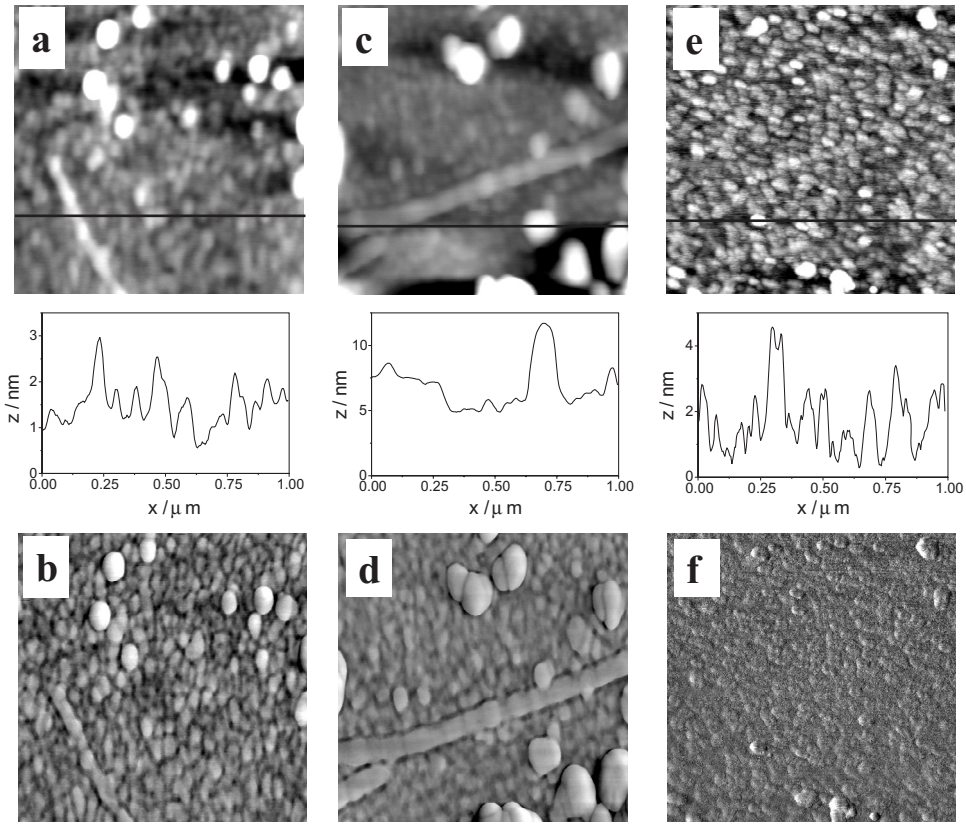

Figure 5. AFM images 1 μm × 1 μm: (a) topography (z = 3.5 nm) with the corresponding cross-section analysis and (b) phase image (z = 1.0 V) of Con A adsorbed onto HXG cast onto amino-terminated surfaces; (c) topography (z = 9 nm) with the corresponding cross-section analysis and (d) phase image (z = 2.5 V) of Con A adsorbed onto TXG cast onto amino-terminated surfaces; (e) topography (z = 4 nm) with the corresponding cross-section analysis and (e) phase image (z = 4.0 V) of Con A adsorbed onto TXG adsorbed onto amino-terminated surfaces.

adsorbed onto pure Si/SiO_2 wafers, carboxymethyl cellulose or cashew gum layers.[25] The presence of XG fibrils and aggregates can still be observed, when the XG surfaces were prepared by casting (Figures 5a and 5c), this show that Con A molecules adsorbed predominantly on the areas free of fibrils and aggregates. XG fibrils and aggregates present strong intermolecular interactions. Therefore, the number of OH groups free to interact with Con A decreased. Contrarily, Con A molecules seem to adsorb homogeneously onto TXG surfaces prepared by adsorption (Figure 5e). This situation corresponds to the adsorption plateau in Figure 4. Phase images also indicated that Con A molecules cover TXG surfaces prepared by adsorption (Figure 5f) more homogenously than HXG (Figure 5b) or TXG (Figure 5d) surfaces prepared by casting.

Desorption experiments were performed by dipping Con A/HXG and Con A/TXG covered-wafers into pure water for 24 hours. After that period of time, the samples were removed, dried and again analyzed by means of ellipsometry. Negligible changes in mean thickness values have been observed, indicating that the adsorption of Con A onto TXG and HXG layers is irreversible. The strong affinity of ConA for glucose and mannose residues is well

Table 2. Mean thickness values (d) obtained for HXG and TXG immobilized onto amino-terminated Si wafers or onto Si/SiO_2 by adsorption (equilibrium condition) or by casting (non-equilibrium condition) determined by means of ellipsometry

Sample	Method	Substrate	d / nm	r.m.s. / nm*
HXG	Adsorption	Amino-terminated	1.3 ± 0.1	0.8 ± 0.1
TXG	Adsorption	Amino-terminated	1.0 ± 0.1	0.8 ± 0.1
HXG	Casting	Amino-terminated	8 ± 1	1.8 ± 0.1
TXG	Casting	Amino-terminated	6.3 ± 0.8	1.3 ± 0.3
HXG	Casting	Si/SiO_2	3.8 ± 0.9	0.5 ± 0.1
TXG	Casting	Si/SiO_2	2.4 ± 0.4	1.9 ± 0.1

*the corresponding mean surface roughness (rms) values determined from topographic images and PicoScan 5.3.2. software.

reported.[24-27] Spectroscopic studies[27] revealed that the molecular recognition of Con A for mannose and glucose residues stems from these carbohydrates possessing hydroxyl configurations at the 3,4 and 6 carbons. Moreover, the axial OH group at the C2 of the mannose favors the affinity of Con A for this carbohydrate. Since, XG cellulosic backbone at C-6 position carries α-D-xylopyranose units, the recognition of Con A might be for OH groups at the C2 and C3. An interesting feature is that isotherms presented in Figure 4 revealed no preferential adsorption of Con A molecules for TXG- or HXG- covered surfaces, despite the differences in their fine structure.

Conclusions

Xyloglucan chains obtained from *H. courbaril* (HXG) are longer and more rigid than xyloglucan chains from *T. indica* (TXG). Moreover, only HXG molecules present XXXXG oligosaccharides in their composition. These molecular and structural differences led to HXG films, which were thicker than TXG films, regardless, the substrate. However, such differences played no role on the adsorption of lectin Con A, Con A adsorbed similarly onto HXG and TXG surfaces. The assemblies of Con A onto HXG and TXG surfaces are promising tools for the development of diseases diagnosis or kits for sugar (glucose or mannose) detection.

Acknowledgments

The authors thank CNPq (Rede Nanoglicobiotec: Proc #555169/2005-7) and FAPESP (Proc #03/10015-3 and #05/50419-1) for financial support. L.B.R.C. also thanks CNPq for a Ph.D. fellowship. The authors thank Prof. R. C. M. de Paula, Universidade Federal do Ceará, Brazil, for the donation *of H. coubaril* seeds.

References

1. Ebringerová, A.; Hromádková, Z.; Heinze, T. In *Advances in Polymer Science, Polysaccharides I Strucuture, Characterization and Use*; Heinze, T., ed.; Springer-Verlag: Heidelberg, 2005, ch.1.
2. Hayashi, T.; *Ann. Rev. Plant Physiol. Plant Molec. Biol.* **1989**, *40*, 139.
3. Lima, D.U.; Buckeridge, M.S.; *Carbohydr. Polym.* **2001**, *46*, 157.
4. Lima, D.U.; Loh, W.; Buckeridge, M.S.; *Plant Physiol. Biochem.* **2004**, *42*, 389.
5. Morris, S.; Hann, S.; Miles, M.J; *Nanotechnology* **2004**, *15*, 1296.
6. Zhou, Q.; Baumann, M.J.; Brumer, H.; Teeri, T.T.; *Carbohydr. Polym.* **2006**, *63*, 449.
7. Stiernstedt, J.; Brumer, H.; Zhou, Q.; Teere, T.T.; Rutland, M.W.; *Biomacromolecules* **2006**, *7*, 2147.
8. Hanus, J.; Mazeau, K.; *Biopolymers* **2006**, *82*, 59.
9. Sharma, R.; Lusignan, C.P.; *US Patent 2006134799* **2006**.
10. Freitas, R.A.; Martin, S.; Santos, G.L.; Valenga, F.; Buckeridge, M.S.; Reicher, F.; Sierakowski, M.-R.; *Carbohydr. Polym.* **2005**, *60*, 507.
11. Chinnayelka, S.; McShane, J.M.; *J. Fluorescence* **2004**, *14*, 585.
12. Bies, C., Lehr, C.-M., Woodley, J.F.; *Adv. Drug Delivery Rev.* **2004**, *56*, 425.
13. Petri, D. F. S.; Wenz, G.; Schunk, P.; Schimmel, T.; *Langmuir* **1999**, *15*, 4520.
14. Fujimoto, J.; Petri, D. F. S.; *Langmuir* **2001**, *17*, 56.
15. Suhara, T.; Fukui, H.; Yamaguchi, M.; *Colloids Surf., A* **1995**, *101*, 29.
16. Iler, R.K.; *The Chemistry of Silica*, Wiley & Sons Publishers: New York, 1979.
17. Brewer, C.; Brown, R.; Koenig, S.; *Biochemistry* **1983**, *22*, 3691.
18. Bhattacharyya, L.; Brewer, C.; Brown, R.; Koenig, S.; *Biochemistry* **1985**, *24*, 4985.
19. Motschmann, H.; Stamm, M.; Toprakcioglu, C.; *Macromolecules* **1991**, *24*, 3681.
20. Azzam, R. M. A.; Bashara N. M.; *Ellipsometry and Polarized Light,* North Holland Publication: Amsterdan, 1987.
21. Ortega-Vinuesa, J.L.; Tengvall, P.; Lundström, I.; *Thin Solid Films* **1998**, *324*, 257.
22. Petri, D. F. S.; *J. Braz.Chem. Soc.* **2002**, *13*, 695.
23. Maganov, S. *In Applied Scanning Probe Methods*; Bhushan, B.; Fuchs, H.; Hosaka, S., eds.; Springer Verlag: Heidelberg, 2004, ch. 7.
24. Reeke Jr, G. N.; Becker, J. W.; Edelman, G. M.; *J. Biol. Chem.* **1975**, *250*, 1525.
25. Castro, L. B. R.; Petri, D. F. S.; *J. Nanosci. Nanotech.* **2005**, *5*, 2063; Castro, L. B. R.; Kappl, M.; Petri, D. F. S.; *Langmuir* **2006**, *22*, 3757; Maciel, J. S.; Kosaka, P. M.; Paula, R. C. M.; Feitosa, J. P. A.; Petri, D. F., S., *Carbohyd. Polym* **2007**, *69*, 522.
26. Smith, E. A.; Thomas, W. D.; Kiessling, L. L.; Corn, R. M.; *J. Am. Chem. Soc.* **2003**, *125*, 6140.
27. Revell, D. J.; Knight, J. R.; Blyth, D. J.; Haines, A. H.; Russel, D. A.; *Langmuir* **1998**, *14*, 4517.

Received: December 8, 2006
Web Release Date: August 15, 2007

FAPESP helped in meeting the publication costs of this article.